

# Investigation of the electrochemical behaviour and surface chemistry of a Ti-13Nb-13Zr alloy exposed in MEM cell culture media with and without the addition of H<sub>2</sub>O<sub>2</sub>

M. A. Baker,<sup>a\*</sup> S. L. Assis,<sup>b</sup> R. Grilli<sup>a</sup> and I. Costa<sup>b</sup>

Promoting and understanding the formation of hydroxyapatite (HA) on biocompatible metals in the body is a very important topic of biomaterials research. In this paper, the formation of HA on a near- $\beta$  Ti-13Nb-13Zr alloy by immersion in minimal essential medium (MEM) with and without the addition of H<sub>2</sub>O<sub>2</sub> has been studied using electrochemical methods, SEM and XPS. The Ti-13Nb-13Zr alloy exhibits passive behaviour over a wide potential range when immersed in MEM, and the passive film is composed of an inner barrier layer and an outer porous layer. Exposure for 72 h in the MEM solution results in the formation of a surface layer composed of an island-like distribution of HA material and adsorbed amino acids. The addition of H<sub>2</sub>O<sub>2</sub> to the MEM solution strongly promotes the formation of a thicker, continuous nanocomposite layer of HA and amino acids. For Ti alloys, the release of H<sub>2</sub>O<sub>2</sub> in the anti-inflammatory response appears to be an important beneficial process, as it serves to accelerate osseointegration. Copyright © 2008 John Wiley & Sons, Ltd.

**Keywords:** XPS; electrochemistry; Ti-13Nb-13Zr alloy; MEM; H<sub>2</sub>O<sub>2</sub>

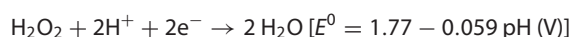
## Introduction

Titanium alloys are used as implant materials owing to their good mechanical properties, corrosion resistance and biocompatibility. Improving the performance of these materials and understanding interfacial interactions with physiological fluids are subjects of much research. Two general reviews on the surface modification and studies of surface interactions for Ti and Ti alloys in biomedical applications have been given by Jones<sup>[1]</sup> and Liu *et al.*<sup>[2]</sup>

Ti-13Nb-13Zr is an alloy developed in the 1990s specifically for biomedical applications. It has good corrosion resistance and biocompatibility and an elastic modulus similar to that of bone.<sup>[3]</sup> Yu and Scully found that both in a simulated physiological solution (Ringer's solution) and a simulated occluded cell environment (5 M HCl),  $\beta$ -Ti-13Nb-13Zr exhibits improved corrosion resistance when compared to other implant alloys such as cp-Ti or Ti-6Al-4V.<sup>[3]</sup>

It is well known that calcium compounds deposited onto the surfaces of Ti alloys [especially hydroxyapatite (HA)] promote osseointegration. There is general agreement that on the outer surface of the passive film of Ti, the formation of a rougher gel-like layer with a high surface area and increased concentration of Ti-OH surface species is important in promoting the growth of apatite.<sup>[1,2]</sup>

Hydrogen peroxide (H<sub>2</sub>O<sub>2</sub>) can stimulate the growth of a hydrated Ti oxide surface layer. H<sub>2</sub>O<sub>2</sub> is a well-known oxidising agent, promoting the corrosive cathodic reaction,



resulting in an enhanced corrosion/oxidation rate.<sup>[4,5]</sup> Exposure to H<sub>2</sub>O<sub>2</sub> causes a thickening and roughening of the oxide on Ti.<sup>[6]</sup> Implantation of materials into the body causes an inflammatory

response, and the generation of H<sub>2</sub>O<sub>2</sub> by inflammatory cells into the extra-cellular space is an accepted biochemical mechanism.<sup>[4]</sup> Tengvall *et al.*<sup>[4,5]</sup> have proposed that the end-product of Ti being implanted into the body is the formation of a duplex oxide with a mostly TiO<sub>2</sub> inner layer and stable hydrated TiOOH gel-like oxide outer layer with good ion and protein exchange properties. Proteins, proteoglycans, inorganic ions and other macromolecules will be incorporated into this gel-like outer layer and provide a surface to which fibroblast and osteoblast cells readily attach.<sup>[5]</sup>

In this study, the corrosion behaviour and surface chemistry of a Ti-13Nb-13Zr alloy immersed in minimal essential medium (MEM), both with and without the addition of H<sub>2</sub>O<sub>2</sub>, have been investigated using electrochemical impedance spectroscopy (EIS), XPS and SEM. The work aims to examine the apatite-forming ability of this Ti alloy in biological media and provide information on the surface chemical processes taking place in the body at the implant-tissue interface.

## Experimental

A near- $\beta$  Ti-13.2Nb-13.5Zr alloy was prepared by arc melting (99.9%) pure Ti and Nb, together with Zr containing 4.5% Hf, under

\* Correspondence to: M. A. Baker, The Surface Analysis Laboratory, Faculty of Engineering and Physical Sciences, University of Surrey, Guildford, Surrey, GU2 7XH, UK. E-mail: m.baker@surrey.ac.uk

a M. A. Baker, R. Grilli The Surface Analysis Laboratory, Faculty of Engineering and Physical Sciences, University of Surrey, Guildford, Surrey, GU2 7XH, UK

b S. L. Assis, I. Costa IPEN/CNEN-SP, Av. Prof. Lineu Prestes 2242, CEP 05508-900, São Paulo, Brazil

argon, using a non-consumable electrode.<sup>[7]</sup> To homogenise the material, it was heat-treated at 1000 °C. For electrochemical tests, the sample surface was mechanically polished to a 1 µm diamond finish. An area of 0.33 cm<sup>2</sup> was exposed to the electrolyte. The MEM solution (a solution composed of salts, amino acids, vitamins and other components essential to cellular growth) was naturally aerated at 37 °C and the pH was maintained at 7.6 with the addition of NaHCO<sub>3</sub>. For one batch of samples, 100 mM of H<sub>2</sub>O<sub>2</sub> was added to the MEM solution. The samples remained immersed in the MEM solution (with or without H<sub>2</sub>O<sub>2</sub>) for 72 h. At this point, some samples were removed for XPS analysis and others underwent EIS and linear polarisation tests.

A three-electrode cell arrangement was used for the electrochemical measurements, with a saturated calomel electrode (SCE) as reference and a platinum wire as the auxiliary electrode. All the potentials measured are referenced to the SCE. Potentiodynamic polarisation scans were carried out at a scan rate of 0.1 mV/s in the range from -800 to 3000 mV using an EG&G273A potentiostat. The EIS tests were undertaken using a Solartron Model SI 1255 frequency response analyser coupled to a Princeton Applied Research (PAR) Model 273A potentiostat/galvanostat. The EIS measurements were obtained at the open circuit potential in a frequency range between 10<sup>5</sup> and 10<sup>-2</sup> Hz with an applied a.c. signal of 10 mV, and at a data collection rate of six points per decade. The temperature was maintained at 37 °C by immersing the 200 ml electrochemical cells in a thermostatic bath. Data fitting of the EIS experimental results to the equivalent circuit was performed using the Zview software.

X-ray (XPS) spectra were recorded on a VG Scientific ESCALAB mk II instrument employing a non-monochromated Al K $\alpha$  source running at 340 W power and a spherical sector analyser. Owing to the low concentration of many elements, survey spectra of the bulk coating were then recorded at 100 eV pass energy and narrow scans at 50 eV pass energy (step width of 0.1 eV). The take-off angle was 45°. Curve-fitting was performed using a mixed Gaussian-Lorentzian lineshape and the spectra were

quantified using instrument-modified Wagner sensitivity factors after a Shirley background subtraction. The spectra were charge-referenced by assigning the adventitious C 1s peak to 285.0 eV.

## Results

A polarisation curve for the Ti-13Nb-13Zr alloy recorded after 72 h immersion in the MEM solution is shown in Fig. 1(a). The Ti alloy exhibits passive behaviour over a large voltage range. From the corrosion potential (approximately -700 mV), as the voltage is swept anodically, the current initially increases steadily until at about 300 mV a plateau is reached and a passive current density ( $i_{pp}$ ) values of 5 µA/cm<sup>2</sup> was observed in the voltage range of 300–1300 mV. At approximately 1300 mV, the current density increased again and stabilised at a value of 25 µA/cm<sup>2</sup> for potentials above 1700 mV. Examination of the surface with SEM showed no evidence of pitting. Yu *et al.*<sup>[3]</sup> have reported that pitting in chloride solutions is not found on Ti alloys up to very high anodic potentials; hence the current density increase at approximately 1300 mV could be either associated with the oxygen evolution reaction or a change in the valence state of one of the cationic species.

Figure 1(b) shows the experimental and fitted Bode diagram data for the Ti-13Nb-13Zr alloy after 72 h in MEM at 37 °C. The high phase angles (around -80°) in a wide frequency range (from 100 to 0.01 Hz) and the high impedance (10<sup>6</sup> Ω cm<sup>2</sup>) at low frequencies suggest a highly capacitive behaviour, typical of passive materials. The oxide layer is providing good corrosion protection of the underlying metal.

On the basis of the work of Kolman and Scully,<sup>[8]</sup> the equivalent electric circuit used is shown in Fig. 1(c). Two constant phase elements ( $CPE_p$  and  $CPE_b$ ) are in parallel with resistances  $R_p$  and  $R_b$ , respectively. It has been proposed that the oxide layer on titanium and titanium alloys has a duplex structure composed of an inner barrier layer and an external porous layer.<sup>[9,10]</sup> In the equivalent

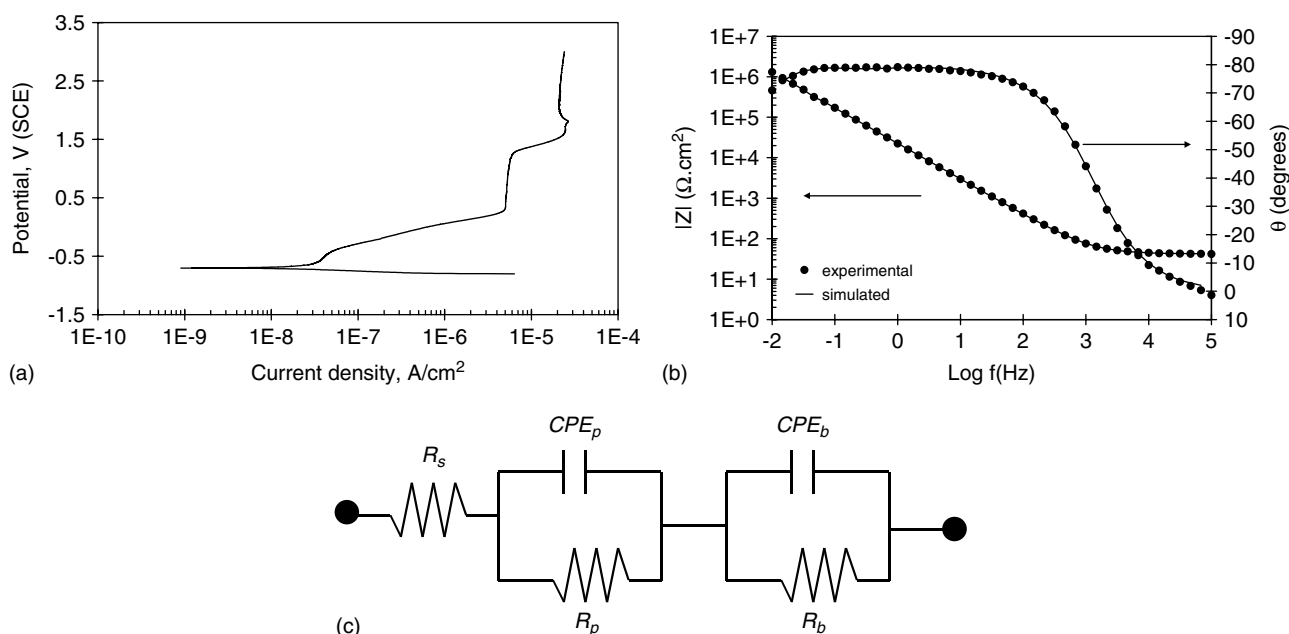


**Figure 1.** (a) Potentiodynamic polarisation curve of Ti-13Nb-13Zr alloy after 72 h immersion in MEM at 37 °C. Scan rate: 0.1 mV/s. (b) EIS Bode diagrams obtained for the Ti-13Nb-13Zr alloy after 72 h in MEM at 37 °C. (c) Equivalent electric circuit used for fitting the EIS data in Fig. 1(b).

circuit,  $CPE_b$  and  $R_b$  represent the capacitive and resistive behaviour of the barrier layer and  $CPE_p$ , and  $R_p$ , the same for the porous layer. It is the barrier layer which affords the good corrosion resistance of titanium alloys.<sup>[8]</sup> The capacitance of the barrier layer,  $CPE_b$ , is responsible for the high phase angles at low frequencies, whereas the electronic and ionic resistance of the barrier layer,  $R_b$ , is responsible for the semi-conductive properties of this layer. The porous layer is highly defective and contains microscopic pores where species from the electrolyte can become incorporated.

The XPS elemental compositions for the Ti-13Nb-13Zr alloy after the different exposures (i) as-received (reference), (ii) exposed to MEM at the free corrosion potential for 72 h and (iii) exposed to MEM + 100 mM H<sub>2</sub>O<sub>2</sub> at the free corrosion potential for 72 h are given in Table 1. The Ti 2p peaks for each of these exposures are shown in Fig. 2(a).

The C 1s peak shape was comparable for all samples, and there was no indication of a substantial carbonate peak being present. For the as-received Ti-13Nb-13Zr alloy, the Ti 2p<sub>3/2</sub>, Zr 3d<sub>5/2</sub> and

Nb 3d<sub>5/2</sub> peaks occur at 485.6, 182.6 and 207.2 eV, respectively, corresponding to the expected binding energies for TiO<sub>2</sub>, ZrO<sub>2</sub> and Nb<sub>2</sub>O<sub>5</sub>, respectively.<sup>[11]</sup> In addition to the small Ti 2p<sub>3/2</sub> metal peak at 453.9 eV, and the predominant TiO<sub>2</sub> peak at 458.6 eV, curve-fitting of the Ti 2p<sub>3/2</sub> peak envelope required two small peaks at 455.3 and 456.6 eV, indicating the presence of small concentrations of TiO and Ti<sub>2</sub>O<sub>3</sub> at the metal/oxide interface.<sup>[12]</sup> The XPS-determined Ti/Nb and Ti/Zr cationic ratios in the oxide were determined to be 12.7 and 10.9 compared to 10.8 and 10.4, respectively, for the bulk. Hence, the cationic concentrations of Zr and Nb in the oxide are remarkably similar to their bulk concentrations. An O 1s peak-fit for the as-received sample is shown in Fig. 2(b). The three components present correspond to oxide at 530.2 eV, an outer hydroxide layer at 531.7 eV and adsorbed water at 533.0 eV. The XPS N 1s peak occurred at 400.2 eV. The peak energy and low intensity are typical of atmospheric contamination.

The specimens exposed to the MEM solution (without H<sub>2</sub>O<sub>2</sub>) also show the formation of TiO<sub>2</sub>, Nb<sub>2</sub>O<sub>5</sub> and ZrO<sub>2</sub> on the

Samples	Ti	Zr	Nb	O	Ca	P	N	Na	C
Ti-13Nb-13Zr (as-received)	7.6	0.7	0.6	30.4	–	–	2.1	–	58.6
Exposed in MEM for 72 h	9.0	1.0	0.9	40.0	2.4	1.8	3.9	1.2	39.8
Exposed in MEM + H <sub>2</sub> O <sub>2</sub> for 72 h	0.4	0.1	0.1	38.5	6.4	6.2	6.6	0.6	41.3

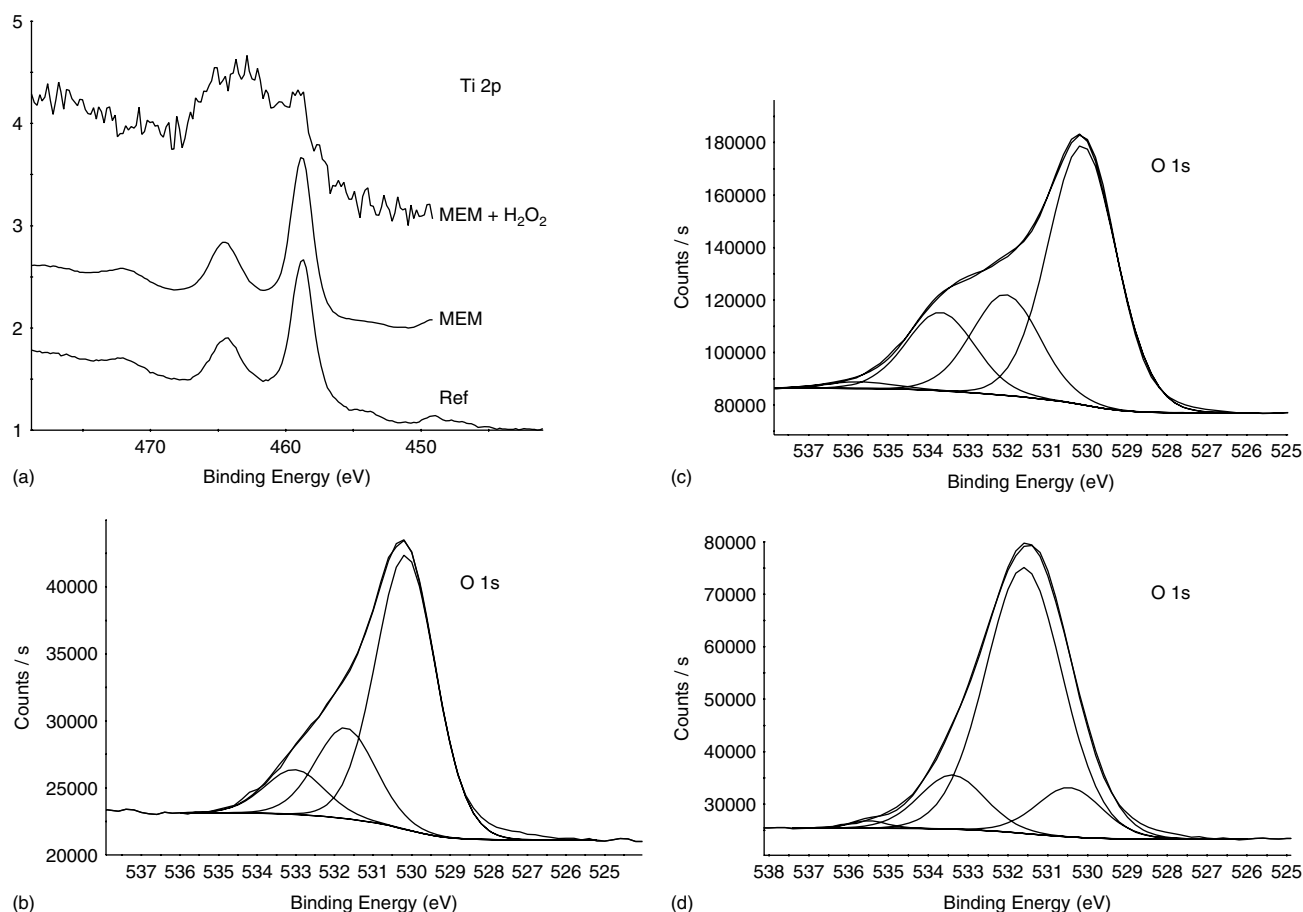


**Figure 2.** (a) XPS Ti 2p peaks for the Ti-13Nb-13Zr alloy exposed to different conditions. (b) XPS O 1s peak-fit for the as-received sample. (c) XPS O 1s peak-fit for sample exposed to the MEM solution (without H<sub>2</sub>O<sub>2</sub>). (d) XPS O 1s peak-fit for sample exposed to the MEM + H<sub>2</sub>O<sub>2</sub> solution.

Ti-13Nb-13Zr alloy. The Ti/Nb and Ti/Zr cationic ratios are 10.0 and 9.0, respectively. The O 1s peak shape (Fig. 2(c)) indicates that the surface formed in MEM solution is more hydrated than that on the air-formed oxide, with an increase in both the OH<sup>-</sup> and H<sub>2</sub>O component intensities. There is a small Na Auger KL<sub>1</sub>L<sub>23</sub> peak at high binding energies. Ca and P are present at approximately 2 at.%, and the P 2p<sub>3/2</sub> and Ca 2p<sub>3/2</sub> peaks occur at 133.4 and 347.6 eV, respectively, corresponding to those expected for HA.<sup>[13,14]</sup> During XPS spectral acquisition, some differential charging was observed, suggesting incomplete formation of an HA surface layer (e.g. an island-like distribution). The nitrogen concentration increased to 4–5 at.%.

The addition of H<sub>2</sub>O<sub>2</sub> to the MEM solution has a dramatic effect on the surface chemistry. Compared to the pure MEM solution, the Ti concentration is strongly reduced from about 8 to 0.4 at.%, with a concomitant increase in the Ca and P concentrations from approximately 2 to 6 at.%. Clearly, a thick HA layer has been deposited. The Ti 2p peak in Fig. 2(a) exhibits poor signal/noise, but there is clearly a peak corresponding to TiO<sub>2</sub>. The total Ti 2p peak envelope appears to extend over a similar binding energy range as the MEM exposed sample, but surprisingly, there is no drop in the intensity between the Ti 2p<sub>3/2</sub> and Ti 2p<sub>1/2</sub> peaks. The O 1s peak (Fig. 2(d)) shows the presence of a principal component at 531.6 eV, corresponding to PO<sub>4</sub><sup>2-</sup>/OH<sup>-</sup> groups of HA, and two smaller peaks at 530.4 and 533.4 eV associated with O<sup>2-</sup> and H<sub>2</sub>O, respectively, consistent with other work.<sup>[14]</sup> Exposure to the MEM + H<sub>2</sub>O<sub>2</sub> media leads to an increase in the nitrogen concentration at the surface to approximately 8 at.% and a shift in the N 1s binding energy to 399.8 eV.

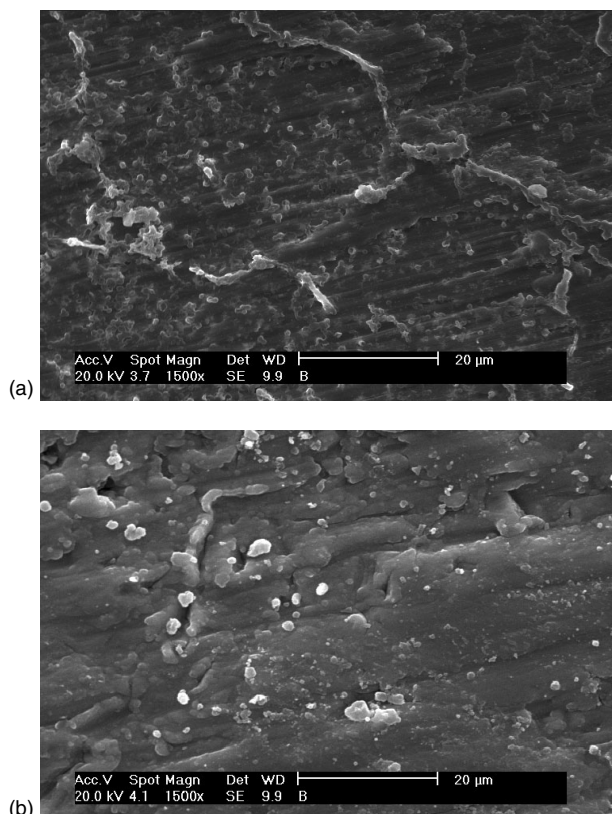


**Figure 3.** SEM micrographs of Ti-13Nb-13Zr alloy after 125 days immersion in MEM: (a) without H<sub>2</sub>O<sub>2</sub>, (b) with 100 mM H<sub>2</sub>O<sub>2</sub>.

SEM images of the Ti-13Nb-13Zr alloy surfaces after 125 days exposure in the MEM and MEM + H<sub>2</sub>O<sub>2</sub> solutions are given in Fig. 3. In the MEM solution, the large number of discrete particles on the surface is representative of the island-like deposition of HA. For the sample exposed in the MEM + H<sub>2</sub>O<sub>2</sub>, the polishing marks on the metal are no longer visible and a generally smoother morphology is observed, indicative of thicker layer formation.

## Discussion

The native oxide formed on the near- $\beta$  Ti-13Nb-13Zr alloy is composed mainly of TiO<sub>2</sub>, but also Nb<sub>2</sub>O<sub>5</sub> and ZrO<sub>2</sub>. The cationic ratios in the oxide are very similar to the bulk, indicating little or no preferential oxide formation. Immersion in the MEM solution results in passive film thickening on the Ti-13-Nb-13Zr alloy surface and passivity is maintained over a large potential range. The EIS results indicate that the passive film is composed of an inner barrier layer and an outer porous layer. The XPS results show that immersion in the MEM solution leads to a small amount of HA being deposited at the surface. The HA has an island-like distribution. From the XPS and SEM results, it is apparent that the addition of H<sub>2</sub>O<sub>2</sub> to the MEM solution results in the formation of a much thicker continuous HA layer.

The shape of the Ti 2p peak envelope for the samples exposed to MEM + H<sub>2</sub>O<sub>2</sub> possibly suggests the presence of components with binding energies higher than that of TiO<sub>2</sub>. In this HA environment, such a high binding energy 2p peak might be expected if the Ti<sup>4+</sup> cation is bonded to groups such as PO<sub>4</sub><sup>3-</sup> or HPO<sub>4</sub><sup>2-</sup><sup>[15]</sup> or as TiOOH,<sup>[16]</sup> rather than O<sup>2-</sup> ions. Consequently, the Ti may become incorporated into the HA-type layer, substituting for Ca cations within the structure<sup>[17]</sup> and/or a TiOOH layer may form at the outer surface of the Ti alloy oxide.<sup>[5]</sup> Further work is required to resolve the exact chemical state and location of Ti cations within this surface region.

XPS N 1s intensities are often used as indicators of amino acid and protein adsorption in studies of biomolecular adsorption onto surfaces. The observed increase in N concentration in the MEM and MEM + H<sub>2</sub>O<sub>2</sub> exposures and the shift of the N peak position to lower binding energy values (corresponding to C–N or amine bonding) are indicative of a layer growing on the surface that is composed both of HA and amino acids. Immersion of the Ti-13Nb-13Zr alloy in MEM solution results in the formation of a surface layer composed of an island-like distribution of HA material and adsorbed amino acids. The addition of H<sub>2</sub>O<sub>2</sub> to the MEM solution strongly promotes the formation of a nanocomposite layer of HA and amino acids. The reactions at the Ti oxide surface that are stimulated by the presence of H<sub>2</sub>O<sub>2</sub> are complex,<sup>[5,6]</sup> but the end result is the growth of a thicker, continuous nanocomposite layer with an overall composition similar to that formed in pure MEM solution. Hence, for Ti alloys, release of H<sub>2</sub>O<sub>2</sub> in the anti-inflammatory response is an important beneficial process, as it serves to accelerate osseointegration.

Importantly, the results presented here show that as HA grows to form a thicker and continuous layer, amino acids continue to be incorporated in that layer. For Ti alloy implant surfaces in the body, in addition to amino acids, the extra-cellular material contains important proteins, such as proteoglycans and collagen. Considering that the island-like formation of HA is relatively slow and it is well known that amino acids and proteins adsorb onto surfaces in a matter of seconds, it is to be expected that such amino

acids and proteins will become incorporated into the growing HA layer, forming a nanocomposite material which favours fibroblast and osteoblast growth.

## Conclusions

1. The native oxide formed on the near- $\beta$  Ti-13-Nb-13Zr alloy is composed mainly of TiO<sub>2</sub>, but also Nb<sub>2</sub>O<sub>5</sub> and ZrO<sub>2</sub>. The cationic ratios in the oxide are very similar to those in the bulk, indicating that no preferential oxidation takes place for this alloy.
2. The near- $\beta$  Ti-13-Nb-13Zr alloy exhibits passivity over a large potential range when immersed in MEM solution. The passive film is composed of an inner barrier layer and an outer porous layer.
3. Exposure for 72 h in the MEM solution results in the formation of a surface layer comprising an island-like distribution of HA material and adsorbed amino acids. The addition of H<sub>2</sub>O<sub>2</sub> to the MEM solution strongly promotes the formation of a thicker, continuous nanocomposite layer of HA and amino acids.
4. For Ti alloys, the release of H<sub>2</sub>O<sub>2</sub> in the anti-inflammatory response is an important beneficial process, as it serves to accelerate osseointegration.

## References

- [1] Jones FH. *Surf. Sci. Rep.* 2001; **42**: 75.
- [2] Lu X, Chu PK, Ding C. *Mater. Sci. Eng., R* 2004; **47**: 49.
- [3] Yu SY, Brodrick CW, Ryan MP, Scully JR. *J. Electrochem. Soc.* 1999; **146**: 4429.
- [4] Tengvall P, Lundström I, Sjöqvist L, Elwing H, Bjursten LM. *Biomaterials* 1989; **10**: 166.
- [5] Tengvall P, Lundström I. *Clin. Mat.* 1992; **9**: 115.
- [6] Pan J, Liao H, Leygraf C, Thierry D, Li J. *J. Biomed. Mater. Res.* 1998; **40**: 244.
- [7] Schneider SG. Processing and characterization of a Ti-13Nb-13Zr alloy for Biomedical Applications, PhD Thesis, Instituto de Pesquisas Energéticas e Nucleares, Sao Paulo, Brazil, 2001.
- [8] Kolman DG, Scully JR. *J. Electrochem. Soc.* 1994; **141**: 2633.
- [9] Lavos-Valereto IC, Ramires I, Guastaldi AC, Costa I, Wolyneć I. *J. Mater. Sci. – Mater. Med.* 2004; **15**: 55.
- [10] Pan J, Thierry D, Leygraf C. *Electrochim. Acta* 1996; **41**: 1143.
- [11] *NIST X-ray Photoelectron Spectroscopy Database*, version 3.4, <http://srdata.nist.gov/xps/> [last accessed in 2007].
- [12] Baker MA, Assis SL, Higa OZ, Grilli R, Costa I. (in press).
- [13] Massaro C, Baker MA, Consentino F, Ramires PA, Klose S, Milella E. *J. Biomed. Mater. Res.* 2001; **58**: 651.
- [14] Kačiulis S, Mattogno G, Pandolfi L, Cavalli M, Gnappi G, Montenero A. *Appl. Surf. Sci.* 1999; **151**: 1.
- [15] Demri B, Muster D. *J. Mater. Process. Technol.* 1995; **55**: 311.
- [16] Welsh ID, Sherwood PMA. *Phys. Rev. B* 1989; **40**: 6386.
- [17] Leadley SR, Davies MC, Ribeiro CC, Barbosa MA, Paul AJ, Watts JF. *Biomaterials* 1997; **18**: 311.